JOURNAL FOR SOCIAL SCIENCE STUDIES
An International Peer-Reviewed Open Access Journal

ISSN (Online): 3006-2071 | ISSN (Print): 3006-2063
Volume 4 • Issue 4 • August 2026

BIOSYNTHESIS OF Fe_2O_3 NANOPARTICLES USING *MORINGA OLEIFERA* LEAF EXTRACT AND THEIR ANTIMICROBIAL, ANTIOXIDANT, ANTI-INFLAMMATORY, AND ANTIDIABETIC ACTIVITIES

Khitab Ur Rahman[1], Saqiba Riaz[*2], Muhammad Mohsin[3], Mohamamd Munir Akbar[4], Hazrat Bilal[5], Rabail Urooj[6]

[1]*Department of Chemical Engineering and Technology, University: Shandong University of Science and Technology, Qingdao, China*
[*2]*MPhil (Chemistry), Dept. Of Chemistry, University of Karachi*
[3]*University of Education, Lahore, Punjab, Pakistan*
[4]*University of Education, Lahore, Faisalabad campus, Punjab, Pakistan*
[5]*National center of excellence in physical chemistry, University of Peshawar, KPK, Pakistan.*
[6]*Assistant Professor, Department of Environmental Sciences, Sardar Bahadur Khan Women's University, Quetta, Pakistan*

[*2]saqibariaz786@gmail.com

DOI: https://doi.org/10.5281/zenodo.22688086

Keywords
Green synthesis, Nanoparticles, Eco-friendly method, Antimicrobial applications, and Biological applications.

Article History
Received: 28 June 2026
Accepted: 15 August 2026
Published: 31 August 2026

Copyright @Author
Corresponding Author: * Saqiba Riaz

Abstract

Nanotechnology offers sustainable opportunities for developing functional materials for biomedical and antimicrobial applications, while plant-mediated synthesis can reduce reliance on hazardous chemical reagents. In the present study, Fe_2O_3 nanoparticles (Fe_2O_3NPs) were biosynthesized using an aqueous leaf extract of Moringa oleifera Lam. through a simple plant-mediated approach. The synthesized Fe_2O_3NPs were characterized by UV–visible spectroscopy, Fourier-transform infrared spectroscopy (FTIR), scanning electron microscopy (SEM), and energy-dispersive X-ray spectroscopy (EDX). UV–Vis analysis showed a characteristic absorption maximum at 350 nm, while FTIR analysis indicated the involvement of plant-derived functional groups and Fe–O vibrations. SEM revealed predominantly rod/rectangular-shaped nanoparticles with an average size of approximately 65 nm, and EDX confirmed iron and oxygen as the principal elements. Qualitative phytochemical screening of the M. oleifera aqueous extract detected phenols, alkaloids, flavonoids, saponins, terpenoids, tannins, glycosides, steroids, proteins, and oils/fats. The biosynthesized Fe_2O_3NPs exhibited concentration- and/or time-dependent biological activities, including antileishmanial, anti-inflammatory, antioxidant, antidiabetic, protein kinase inhibitory, antibacterial, and antifungal effects. At the highest tested conditions, antileishmanial inhibition reached 71%, anti-inflammatory inhibition 79%,

JOURNAL FOR SOCIAL SCIENCE STUDIES
An International Peer-Reviewed Open Access Journal

ISSN (Online): 3006-2071 | ISSN (Print): 3006-2063
Volume 4 • Issue 4 • August 2026

total antioxidant capacity 78.4%, total reducing power 75.2%, and DPPH radical-scavenging activity 64.6%. α-Amylase and α-glucosidase inhibition reached 55.23 ± 0.35% and 56.59 ± 1.34%, respectively. The maximum antibacterial inhibition zones were 24.0 ± 1.44 mm against Escherichia coli, 22.0 ± 1.45 mm against Pseudomonas aeruginosa, and 21.0 ± 0.26 mm against Staphylococcus aureus, while antifungal inhibition against Ascochyta rabiei reached 70 ± 2.1%. Hemolysis remained low, with a maximum value of 1.46 ± 0.10% at 200 µg/mL. Overall, the findings demonstrate that M. oleifera-mediated Fe_2O_3NPs possess multifunctional biological properties and represent a promising green platform for further investigation in biomedical and antimicrobial applications.

1. Introduction

Nanotechnology is a rapidly advancing interdisciplinary field that integrates principles from biology, chemistry, physics, materials science, and engineering to develop and utilize materials at the nanoscale. Nanoparticles (NPs), generally defined as particles with dimensions between approximately 1 and 100 nm, exhibit distinctive physicochemical characteristics arising from their small size, high surface-area-to-volume ratio, surface reactivity, and tunable morphology [1]. These properties enable nanoparticles to exhibit functionalities that differ substantially from their bulk counterparts, making them attractive for applications in environmental remediation, agriculture, medicine, biotechnology, catalysis, and other emerging technologies [2]. Depending on their composition and structural characteristics, nanoparticles can occur in diverse forms, including nanospheres, nanocrystals, nanoflowers, nanotubes, and nanowires. However, conventional physical and chemical approaches for nanoparticle synthesis may involve high energy consumption, elevated temperatures, hazardous reducing agents, and toxic organic solvents, which can limit their environmental sustainability and biological applicability [3].

In response to these limitations, biological or "green" synthesis has emerged as a promising alternative for the fabrication of nanoparticles. Biological synthesis employs naturally occurring reducing and stabilizing agents derived from microorganisms, algae, and plants [4–7]. Among these approaches, plant-mediated synthesis has attracted particular attention because it is relatively simple, economical, environmentally compatible, and potentially scalable. Plant extracts contain a wide range of bioactive metabolites, including phenolic compounds, flavonoids, terpenoids, alkaloids, proteins, sugars, and other secondary metabolites that can participate in the reduction of metal ions and the subsequent stabilization and capping of newly formed nanoparticles. Unlike microbial systems, plant-mediated synthesis generally does not require the maintenance of aseptic cultures or complex growth conditions, thereby facilitating rapid and comparatively straightforward nanoparticle production [8]. Moreover, the phytochemical composition of plant extracts can influence nanoparticle size, morphology, surface chemistry, stability, and ultimately their biological and catalytic performance.

Among metal and metal oxide nanomaterials, iron oxide nanoparticles have received considerable scientific attention because of their distinctive physicochemical, magnetic, optical, catalytic, and biological properties. Iron oxide nanoparticles, including Fe_2O_3-based nanostructures, have demonstrated considerable potential in environmental, biomedical, agricultural, and industrial applications [9]. Their physicochemical properties, including surface reactivity, magnetic behavior, relatively high chemical stability, and the ability to interact with a wide range of biomolecules, make them attractive candidates for

JOURNAL FOR SOCIAL SCIENCE STUDIES
An International Peer-Reviewed Open Access Journal
ISSN (Online): 3006-2071 | ISSN (Print): 3006-2063
Volume 4 • Issue 4 • August 2026

multifunctional applications [10,11]. In particular, Fe_2O_3 nanoparticles (Fe_2O_3NPs) have been investigated for applications in catalysis, sensing, pigments, environmental remediation, and biomedical technologies [12–14]. Their relatively favorable biocompatibility and potential for surface functionalization further increase their utility in biological systems [15,16]. Importantly, the physicochemical characteristics and biological performance of Fe_2O_3NPs can be strongly influenced by their synthesis route and surface chemistry. Consequently, green synthesis using plant-derived phytochemicals offers an attractive strategy for producing Fe_2O_3NPs with biologically functionalized surfaces while minimizing the use of hazardous chemical reagents.

Plants have long been recognized as valuable sources of bioactive compounds and have been traditionally used as food, medicinal preparations, and therapeutic remedies [17]. Among medicinal and nutritionally important plants, *Moringa oleifera* Lam. has attracted considerable scientific interest because of its rich phytochemical composition and diverse biological properties. *M. oleifera*, commonly known as moringa or the drumstick tree, belongs to the family Moringaceae and is widely cultivated in tropical and subtropical regions. Different parts of the plant, particularly the leaves, seeds, flowers, bark, and pods, contain numerous biologically active constituents. Phytochemical investigations have reported the presence of phenolic acids, flavonoids, glucosinolates, isothiocyanates, alkaloids, terpenoids, tannins, saponins, vitamins, minerals, and other bioactive compounds in *M. oleifera* [18–20]. These constituents have been associated with a broad spectrum of biological activities, including antioxidant, antimicrobial, anti-inflammatory, antidiabetic, hepatoprotective, cardioprotective, and anticancer effects [21–24].

The abundance and diversity of phytochemicals in *M. oleifera* also make this plant a promising biological resource for nanoparticle synthesis. Phenolic compounds, flavonoids, reducing sugars, proteins, and other functional molecules present in *M. oleifera* extracts may facilitate the conversion of precursor ions into nanoparticles and subsequently interact with their surfaces to promote stabilization and capping. Such phytochemical-mediated functionalization may influence nanoparticle aggregation, colloidal stability, surface characteristics, and biological activity. Therefore, the use of *M. oleifera* as a biological reducing and stabilizing system may provide an environmentally friendly route for the synthesis of Fe_2O_3NPs while simultaneously introducing plant-derived surface functionalities that could contribute to their biological performance. Despite the increasing number of reports on plant-mediated nanoparticle synthesis, considerable variation remains in the physicochemical characteristics and biological activities of nanoparticles synthesized using different plant species. In particular, the relationship between the phytochemical constituents of *M. oleifera* and the formation, stabilization, and functional performance of Fe_2O_3NPs requires further investigation. Comprehensive assessment integrating nanoparticle synthesis, physicochemical characterization, and multiple biological assays can provide a more complete understanding of the potential of *M. oleifera*-mediated Fe_2O_3NPs as multifunctional nanomaterials. Such an approach may also help establish a sustainable alternative to conventional nanoparticle synthesis while expanding the biomedical and antimicrobial applications of iron oxide nanomaterials.

Therefore, the present study was designed to develop an eco-friendly and cost-effective method for the green synthesis of Fe_2O_3NPs using *Moringa oleifera* Lam. extract and to systematically evaluate their physicochemical and biological properties. Specifically, the study aimed to: (i) investigate the phytochemical constituents of *M. oleifera* potentially involved in the reduction, capping, and stabilization of Fe_2O_3NPs; (ii) synthesize Fe_2O_3NPs through a plant-mediated approach while minimizing energy consumption and avoiding hazardous chemical reducing agents; (iii)

JOURNAL FOR SOCIAL SCIENCE STUDIES
An International Peer-Reviewed Open Access Journal
ISSN (Online): 3006-2071 | ISSN (Print): 3006-2063
Volume 4 • Issue 4 • August 2026

characterize the synthesized Fe_2O_3NPs using scanning electron microscopy (SEM), energy-dispersive X-ray spectroscopy (EDX), Fourier-transform infrared spectroscopy (FTIR), and UV–visible spectroscopy to determine their morphology, elemental composition, hydrodynamic properties, functional groups, and optical characteristics; (iv) evaluate their antioxidant, biocompatibility, antiparasitic, anti-inflammatory, anticancer, and antidiabetic activities; and (v) assess their antimicrobial efficacy against selected pathogenic bacterial and fungal strains. Collectively, this study seeks to establish *M. oleifera*-mediated Fe_2O_3NPs as multifunctional nanomaterials with potential applications in biomedical and antimicrobial fields and to provide a sustainable platform for plant-assisted nanomaterial synthesis.

2. Materials and Methods

2.1. Chemicals

Ferric chloride ($FeCl_3$, ≥98% purity, Sigma-Aldrich, USA), dimethyl sulfoxide (DMSO, ≥99.5% purity, Merck, Germany), sodium hydroxide (NaOH, ≥98% purity, Sigma-Aldrich, USA), ascorbic acid (AA, ≥99% purity, Sigma-Aldrich, USA), 2,2-diphenyl-1-picrylhydrazyl (DPPH, ≥95% purity, Sigma-Aldrich, USA), methanol (HPLC grade, ≥99.9% purity, Merck, Germany), amphotericin-B (≥95% purity, Sigma-Aldrich, USA), diclofenac sodium (≥98% purity, Sigma-Aldrich, USA), bovine serum albumin (BSA, ≥98% purity, Sigma-Aldrich, USA), Whatman filter paper No. 1 (Whatman International Ltd., UK), and Tris buffer (≥99% purity, Sigma-Aldrich, USA) were used in this study. All chemicals employed were of analytical grade.

2.2. Collection and identification of plant species

The *Moringa oleifera* plant was collected from Jhelum in 2024. The plant was identified using scientific literature [25]. Subsequently, the plant was authenticated through its morphological characteristics and verified by a taxonomist.

2.3. Synthesis of plant extract

The extract was made by collecting *M. oleifera* leaves and vigorously splashing them in running water to remove any dust or other material that might have adhered to their surface. Following cleaning, the leaves were all dried in a shady place and ground into fine particles via a grinder. 250 mL of double-distilled water (DDW) was mixed with the produced powder, heated for 15 min, and then incubated for another 15 min at 80°C in a water bath. After cooling and filtering through muslin cloth and Whatman filter paper, the resulting mixture was set at 4°C. The extract was then stored for further analysis and potential use in various applications.

2.4. Qualitative study on phytochemical constituents of phyto-extract

A qualitative phytochemical study includes the method of detecting and identifying different phytoactive components. It aims to assess the absence or occurrence of particular phytochemicals like flavonoids, phenolic compounds, alkaloids, protein, terpenoids, glycosides, saponins, oils, steroids, quinones, anthocyanins, and tannins. The Qualitative phytochemical assessment was achieved through the previous standard protocol [26].

2.5. Preparation of Fe_2O_3NPs

For the synthesis of Fe_2O_3NPs, 100 mL of *M. oleifera* extract was slowly added to 100 mL of $FeCl_3$ solution. The obtained solution was kept on a hot plate and stirred using a magnetic stirrer at 200 rpm at 100 °C for 6 h. Over time, the solution color was transformed from brownish to dark brown. Then centrifugation was performed for 35 min at 6,000 rpm. Once centrifugation was done, the supernatant was removed, and the NPs were transferred into Petri plates and desiccated via a hot plate at 350 °C. The obtained NPs were then kept at 25 °C. These prepared NPs were confirmed via various spectroscopic and microscopic techniques before their use in different biological assays.

JOURNAL FOR SOCIAL SCIENCE STUDIES
An International Peer-Reviewed Open Access Journal
ISSN (Online): 3006-2071 | ISSN (Print): 3006-2063
Volume 4 • Issue 4 • August 2026

2.6. Characterization of Fe_2O_3NPs

2.6.1. UV-Vis study

The optical properties of the phyto-fabricated Fe_2O_3NPs in solution were analyzed via UV-Vis spectroscopy (Shimadzu UV-1800, Japan) at room temperature. This technique allowed for the determination of the surface plasmon resonance band, which provides insights into the optical properties of the NPs.

2.6.2. SEM and EDX study

SEM was performed to analyze the surface properties of the prepared Fe_2O_3NPs. SEM (JEOL JSM-6380A) was performed at 25 °C following the previously documented protocol [27]. The EDX study was executed to assess the composition, their occurrence proportion, and the determination of the presence of iron and oxygen. EDX (EOL JSM-6380A SEM equipped with an Oxford Instruments EDX detector) was used to assess the qualitative assessment of the constituents in Fe_2O_3NPs in a dispersed manner at 25 °C.

2.6.3. FTIR spectroscopy

FTIR analysis of Fe_2O_3NPs was performed to identify structural characteristics and validate various functional groups. The FTIR examination of the Fe_2O_3NPs sample was prepared following the former standard procedure with a little modification [28], using a Shimadzu IRTracer-100 FTIR spectrophotometer at 25 °C.

2.7. Pharmacological Applications of the Fe_2O_3NPs

2.7.1. Antileishmanial activity

The antiparasitic potential of the prepared NPs was tested against *Leishmania tropica* promastigotes, according to the previous standard procedure [29]. Parasite numbers were counted using a hemocytometer in all tubes, including both NPs treated tubes and control tubes, at different time durations from 24-96 h, and the percentage (%) inhibition was determined using the formula (1):

$$\%\ Inhibition = ((Abs\ control - Abs\ sample)/Abs\ control) \times 100 \quad (1)$$

Where Abs sample denotes the absorbance of the Fe_2O_3NPs-containing sample and Abs control represents the absorbance of the control tube.

2.7.2. Anti-inflammatory assessment

The anti-inflammatory efficiency of the plant extract and Fe_2O_3NPs was assessed using the previously documented protocol [30]. A reaction mixture was prepared with BSA in a saline Tris buffer at pH 6.8. Then, 900 µL of BSA was combined with 100 µL of various concentrations of Fe_2O_3NPs (25, 50, 100, 200, and 400 µg/mL). Diclofenac sodium (in µg/mL) was used as the standard. The assay was performed according to the aforementioned standard protocol, and the absorbance was measured at 580 nm [31]. Protein denaturation was determined using the following equation (2):

$$Protein\ Inhibition\ percentage\ (\%) = ((Abs\ control - Abs\ sample)/Abs\ control) \times 100 \quad (2)$$

Where Absample denotes the absorbance of the Fe_2O_3NPs-containing sample and Abcontrol represents the absorbance of the control tube.

2.7.3. Antioxidant potential

Various antioxidant assays, including total antioxidant capacity (TAC), DPPH-free radical scavenging (FRSA), and total reducing power (TRP), were executed to measure the antioxidant efficacy of Fe_2O_3NPs at several concentrations ranging from 50–200 µg/mL [31]. These assays allowed for a comprehensive evaluation of the Fe_2O_3NPs ' ability to neutralize free radicals and diminish oxidative stress, which is key to their potential therapeutic applications. The results from these assays provide valuable insights into the NPs' effectiveness in combating oxidative damage and their suitability for use in various biomedical fields. Ascorbic acid (AA) and DMSO were applied as positive and negative controls, respectively.

JOURNAL FOR SOCIAL SCIENCE STUDIES
An International Peer-Reviewed Open Access Journal
ISSN (Online): 3006-2071 | ISSN (Print): 3006-2063
Volume 4 • Issue 4 • August 2026

2.7.3.1. TAC assay

To determine TAC, 100 µL of every dose of Fe_2O_3NPs was mixed individually with reagents following the earlier published procedure [31]. AA and DMSO were applied as positive and negative controls, respectively.

2.7.3.2. TRP assay

For the determination of the TRP assay, the potassium-ferricyanide method was utilized [31]. AA and DMSO were applied as positive and negative controls. Then the Absorbance of each sample, including treated and control samples, was measured at 580 nm.

2.7.3.3. FRSA assessment

For FRSA determination, we follow the previously documented standard procedure [31]. Then the percentage (%) inhibition was determined using the subsequent aquation (3):

$$\% \text{ FRSA} = (Abs \text{ control} - Abs \text{ sample}) / Abs \text{ control} \times 100 \quad (3)$$

Where Abs sample shows the nanoparticles-treated sample, and Abs control is the control sample.

2.7.4. Protein (PK) kinase inhibition

The PK inhibition test was executed according to the previous standard protocol with some adjustments [32]. The PK inhibitory assay was used to find the anticancer activity of the bioinspired Fe_2O_3NPs. A Streptomyces 85E strain was cultured to assess the PK inhibition activity of Fe_2O_3NPs. The test organism, *Streptomyces sp.* strain 85E, was obtained from the National Institute of Health. Surfactin was utilized as a positive control. The ZOI was calculated as described previously [33].

2.7.5. Antidiabetic activity

The antidiabetic efficacy of plant-mediated Fe_2O_3NPs was assessed by means of α-glucosidase and α-amylase inhibition assessment. These assays were conducted to gauge the potential of Fe_2O_3NPs in inhibiting the key enzymes involved in carbohydrate digestion, which can help in controlling postprandial blood glucose levels. The results demonstrated the promising antidiabetic properties of Fe_2O_3NPs, indicating their potential as therapeutic agents for managing diabetes.

2.7.5.1. Alpha amylase (AA) inhibition potential assay

A previously published procedure with slight changes was used with little modifications [34]. Acarbose was applied as a positive and deionized water was applied as a negative control, respectively. The % enzyme inhibition was determined via the subsequent equation.

$$\% \text{ inhibition} = ((Abs \text{ negative control} - Abs \text{ sample}) / (Abs \text{ negative control} - Abs \text{ blank})) \times 100 \quad (4)$$

Where Abs Sample is the absorbance of the reaction mixture containing Fe_2O_3NPs and enzyme, Abs negative control is the absorbance of the reaction mixture in deionized water, and Abs Blank is the absorbance without enzyme.

2.7.5.2. Alpha-glucosidase (AG) inhibition potential

The anti-diabetic activity of Fe_2O_3NPs was further evaluated using an alpha-glucosidase inhibition assay based on a previously published procedure with minor changes [35]. Acarbose was applied as a positive control, and deionized water as a negative. The AG inhibition potential was determined using Equation 5.

$$\% \text{ inhibtion} = ((Abs \text{ negative control} - Abs \text{ sample}) / (Abs \text{ negative control} - Abs \text{ blank})) \times 100 \quad (5)$$

Where Abs Sample is the absorbance of the reaction mixture containing Fe_2O_3NPs and enzyme, Abs Negative control is the absorbance of the reaction mixture in deionized water, and Abs Blank is the absorbance without enzyme.

2.7.6. Biocompatibility assay

A hemolytic activity assay was conducted to evaluate the biocompatible nature of the

JOURNAL FOR SOCIAL SCIENCE STUDIES
An International Peer-Reviewed Open Access Journal
ISSN (Online): 3006-2071 | ISSN (Print): 3006-2063
Volume 4 • Issue 4 • August 2026

Fe_2O_3NPs by applying them to fresh RBCs isolated from a healthy donor, following the previously documented procedure [35]. Triton X-100 was used as the positive control, while phosphate-buffered saline (PBS) served as the negative control. After incubation, the sample was centrifuged at 7000 rpm for 22 min. The absorbance was then measured at 500 nm to determine the percentage of hemoglobin release. The percentage of hemolysis was calculated using the following formula (6)

Hemolysis = ((*Abs* sample– *Abs* negative control)/(*Abs* positive control-*Abs* negative control))×100

Where:

Abs sample = absorbance of RBCs treated with Fe_2O_3 NPs

Abs negative control = absorbance of PBS (0% lysis)

Abs positive control = absorbance of Triton X-100 (100% lysis)

2.8. Estimation of the Antimicrobial Potential

2.8.1. Antifungal Assay

To evaluate the antifungal activity, the prepared Fe_2O_3NPs were tested against *Ascochyta rabiei*. The *A. rabiei* culture was obtained from the preserved culture at the National Agriculture Research Center, Islamabad. The preserved *A. rabiei* was re-cultured on potato dextrose agar (PDA) medium and then incubated for one week at 25 ± 1°C. PDA medium was treated with varying doses of Fe_2O_3NPs (0.25, 0.5, 0.75, and 1 mg/mL). A 4 mm disc of *A. rabiei* was placed in the center of the Fe_2O_3NPs-amended Petri plates. Amphotericin B was considered a positive control. The NPs' amended plates were incubated for one week (7 days) at 25 ± 1°C, and the antifungal activity was assessed by applying the subsequent formula.

$$Growth\ Inhibition\ \% = 100 \times \frac{C - T}{C} \quad (7)$$

Where C demonstrates the growth of fungus in a control plate, and T displays the development of fungus in an Fe_2O_3NPs-treated plate.

2.8.2. Antibacterial assay

The antibacterial efficacy was estimated against *S. aureus*, *P. aeruginosa*, and *E. coli*, following a previously established procedure with slight modifications [36]. The bacterial culture was obtained from the preserved culture at the National Agriculture Research Center, Islamabad. The antibacterial assay was performed at various concentrations (200, 100, and 50 µg/mL) in accordance with the standard procedure, with a slight modification [37]. Positive controls with antibiotics (carbapenems) and negative controls containing less than 1% dimethyl sulfoxide (DMSO) were included. The plates were placed in an incubator at 30°C for 24 h, and after incubation, the ZOI were determined in mm.

2.9. Statistical assessment

All samples were collected in triplicate, and statistical investigation was conducted using SPSS version 16.0 and Origin Pro 9. Additionally, data were evaluated for significance to confirm the consistency of the results.

3. Results and Discussion

3.1. Qualitative study of the phytochemicals

The qualitative phytochemical profile of the aqueous extract of *Moringa oleifera* Lam. was evaluated to identify the major secondary metabolites present in the plant extract, as presented in Table 1. The phytochemical screening was performed to detect phenols, alkaloids, flavonoids, saponins, terpenoids, tannins, glycosides, steroids, anthocyanins, quinones, proteins, and oils and fats. The complete qualitative profile is presented in Table 1. The results revealed the presence of several important phytochemical constituents in the aqueous extract of M. *oleifera*. Alkaloids and flavonoids showed strong positive reactions (+++), whereas phenolic compounds exhibited a moderate positive reaction (++). Saponins, terpenoids, tannins, glycosides, steroids, proteins, and oils and fats were detected at lower qualitative levels (+). In contrast, anthocyanins and quinones

JOURNAL FOR SOCIAL SCIENCE STUDIES
An International Peer-Reviewed Open Access Journal
ISSN (Online): 3006-2071 | ISSN (Print): 3006-2063
Volume 4 • Issue 4 • August 2026

were not detected under the experimental conditions used. Minor variations in the phytochemical composition of *M. oleifera* compared with previous reports may be attributed to differences in plant material, geographical origin, environmental conditions, physiological status, maturity, and extraction procedures [38].

The detected phytochemicals are widely recognized for their antioxidant, antimicrobial, and anti-inflammatory properties and may contribute to the biological activity of the plant extract [39]. In addition to their biological significance, phenolic compounds, flavonoids, alkaloids, proteins, and other phytoconstituents may participate in the reduction, capping, and stabilization of Fe_2O_3 nanoparticles during green synthesis. These metabolites can interact with the nanoparticle surface through their functional groups, potentially improving nanoparticle stability and influencing their physicochemical and biological characteristics. Therefore, the phytochemical richness of *M. oleifera* not only supports its traditional and pharmacological importance but also highlights its potential as a natural biofactory for the eco-friendly synthesis of functional Fe_2O_3 nanoparticles [40].

Table 1. Qualitative analysis of the extract of *Moringa oleifera*

Sr. No.	Secondary metabolites	*M. oleifera* aqueous extract
1	Phenols	++
2	Alkaloids	+++
3	Flavonoids	+++
4	Saponins	+
5	Terpenoids	+
6	Tannins	+
7	Glycosides	+
8	Steroids	+
9	Anthocyanins	–
10	Quinones	–
11	Proteins	+
12	Oils and fats	+

3.2. Characterization of Fe_2O_3NPs

3.2.1. UV-Visible Spectroscopy

The plant extract and iron salts are responsible for the nanoparticle's formation. The rapid reaction between the phytochemical constituents of *Moringa oleifera* extract and ferric chloride was indicated by a visible color change from brownish to dark brown, confirming the initiation of iron oxide nanoparticle (Fe_2O_3NPs) formation. The UV–visible absorption spectrum of the prepared nanoparticles exhibited a strong peak at 350 nm (Figure 1). This absorption band corresponds to the surface plasmon resonance (SPR) of iron oxide nanoparticles, which arises due to collective oscillations of electrons on the nanoparticle surface when excited by light. Such a characteristic peak in the 350 nm range has been consistently reported for Fe_2O_3 NPs synthesized using green approaches [41, 42]. The absorption peak around 350 nm in the UV–Vis spectrum indicates the characteristic optical transition of Fe_2O_3 nanoparticles, confirming their formation. This shift from bulk material absorption highlights the nanoscale nature and successful synthesis of Fe_2O_3 NPs [43]. The sharpness and intensity of the peak at 350 nm suggest the nanoparticles are well-dispersed with minimal aggregation of the synthesized Fe_2O_3NPs [44]. Previous studies have shown that shifts in absorption maxima are

JOURNAL FOR SOCIAL SCIENCE STUDIES
An International Peer-Reviewed Open Access Journal
ISSN (Online): 3006-2071 | ISSN (Print): 3006-2063
Volume 4 • Issue 4 • August 2026

influenced by particle size, crystallinity, and capping molecules present in the plant extract [45].

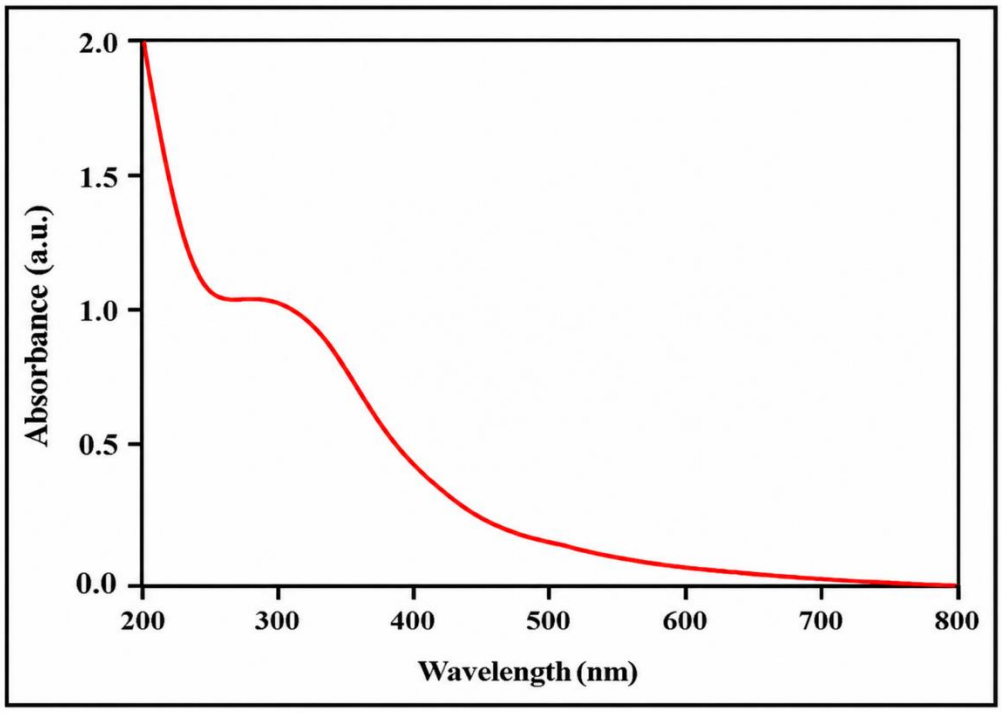

Figure 1. UV of phyto-fabricated Fe_2O_3NPs.

3.2.2. FTIR Spectroscopy

The FTIR spectrum of the biosynthesized Fe_2O_3 (Figure 2) displayed a broad absorption band around ~3400 cm^{-1} corresponding to O–H stretching and hydrogen-bonded hydroxyl groups, weak signals at 2920–2850 cm^{-1} from aliphatic C–H stretching, and a distinct band at ~1630–1650 cm^{-1} attributed to C=O stretching or H–O–H bending. Additional peaks appeared between ~1380–1450 cm^{-1} (C–H bending/–CH_3 deformation or residual –NO_3) and ~1100–1000 cm^{-1} (C–O and C–O–C stretching of alcohols/ethers), while strong absorptions in the fingerprint region at ~570–590 cm^{-1} and ~420–460 cm^{-1} confirmed Fe–O stretching vibrations typical of iron oxide. These features verify successful nanoparticle formation and indicate that organic moieties from the plant extract remain associated with the surface, functioning as reducing and stabilizing agents. The retention of organic peaks suggests phytochemical capping, which enhances dispersion stability and may influence biological activity. Similar FTIR profiles have been reported for green-synthesized iron-oxide nanoparticles using plant extracts, where O–H, C=O, and C–O bands arise from phenolics, flavonoids, proteins, and polysaccharides, and Fe–O vibrations consistently occur within the 400–600 cm^{-1} range [46]. Minor variations in Fe–O peak positions or intensity across studies are typically due to differences in plant metabolites, particle size, crystalline phase (Fe_2O_3), or synthesis conditions [47]. Compared with calcined or extensively washed nanoparticles in earlier reports, which often show diminished organic signals, the strong phytochemical bands in Fe_2O_3 highlight that biomolecular capping was preserved, a feature advantageous for biomedical and catalytic applications. This finding is in agreement with reports by Amutha and Sridhar, who observed

JOURNAL FOR SOCIAL SCIENCE STUDIES
An International Peer-Reviewed Open Access Journal

ISSN (Online): 3006-2071 | ISSN (Print): 3006-2063
Volume 4 • Issue 4 • August 2026

similar Fe–O stretching peaks and phytochemical signatures in plant-mediated Fe_2O_3 nanoparticles [48]. In contrast, studies using thermal or chemical synthesis often lack these organic bands, reflecting the absence of natural capping agents [49]. Therefore, the current results emphasize the advantages of green synthesis, where retained phytochemicals not only stabilize the nanoparticles but also impart potential bioactivity, making them superior to conventionally synthesized counterparts [50].

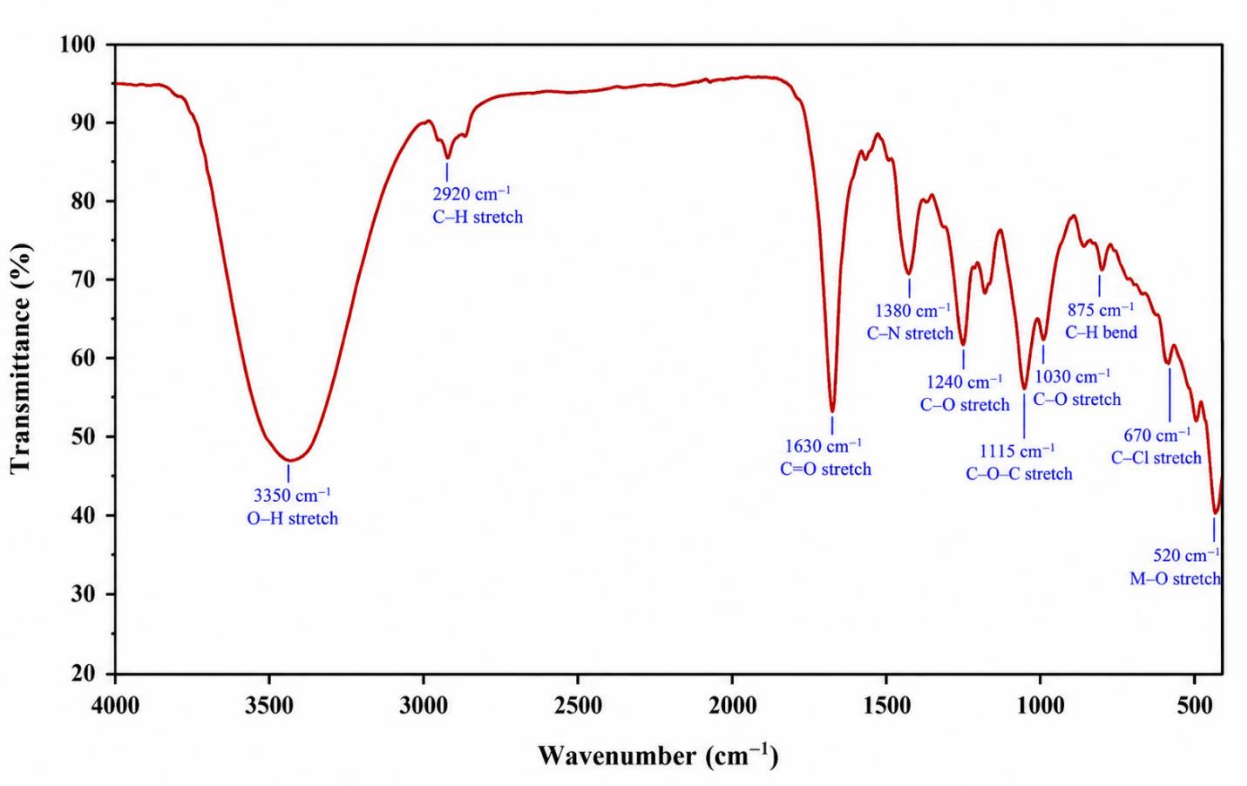

Figure 2. FTIR spectroscopy of phyto-fabricated Fe_2O_3NPs

3.2.3. SEM and EDX spectroscopy

SEM was performed to inspect the structural configuration and dispersion of the Fe_2O_3NPs. The surface properties were clearly observed through SEM analysis (Figure 3A). The SEM micrograph confirmed that the Fe_2O_3NPs appeared as white-colored particles with a rod-shaped morphology having an average size of 65 nm, arranged in a clustered or clumped manner. The predominance of rectangular (rod)-shaped nanoparticles suggests controlled nucleation and growth during the biosynthesis process, likely mediated by the phytochemicals in *M. oleifera* extract, which acted as natural capping agents. Such bioactive compounds prevent excessive aggregation and help maintain shape integrity. The rod-shaped morphology observed in this study provides strong evidence for successful nanoparticle formation and allows assessment of surface topography, size distribution, and aggregation tendencies. While some degree of clustering is expected in biologically synthesized nanoparticles due to the presence of organic molecules on their surface, the relatively uniform shape and size indicate effective stabilization by plant-derived metabolites. Similar morphological characteristics have been reported for green-synthesized Fe_2O_3 nanoparticles in earlier studies [51, 52], further validating our results. Moreover, particle aggregation, as seen in clusters, can also be

JOURNAL FOR SOCIAL SCIENCE STUDIES
An International Peer-Reviewed Open Access Journal

ISSN (Online): 3006-2071 | ISSN (Print): 3006-2063
Volume 4 • Issue 4 • August 2026

attributed to magnetic interactions among iron oxide nanoparticles, a common phenomenon that influences their surface energy and dispersibility [53].

The elemental composition of the prepared NPs was inspected by means of the EDX study. The EDX study of the Fe_2O_3NPs established the existence of iron (Fe) and oxygen (O), verifying the formation of Fe_2O_3NPs, along with traces of other impurities such as carbon and sodium, likely originating from the plant extract (Figure 3B). The weight percentages of Fe and O were found to be 35.0% and 17.9%, respectively. These findings align with previous studies conducted by nanotechnologists [54]. Additionally, the EDS elemental distribution was examined. Figure 4 shows that the NPs are uniformly dispersed on the carbon foil. These results highlight the ability of the EDX detector to rapidly identify Fe_2O_3NPs. The uniform distribution of signals further supports the purity of the nanoparticles' elemental core, while the trace signals can be attributed to organic residues from the plant matrix or the carbon grid used for sample mounting [55]. These results highlight the capability of the EDX detector to rapidly identify Fe_2O_3NPs and confirm their formation with surface-stabilizing biomolecules characteristic of plant-mediated synthesis.

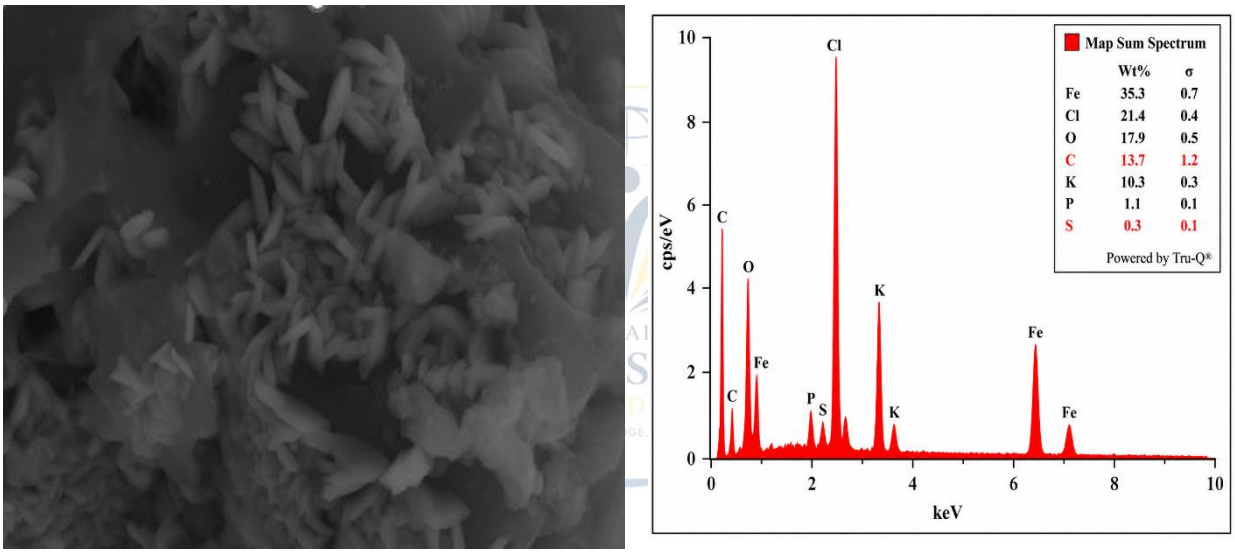

Figure 3. SEM micrograph (A) and EDX study (B) of phyto-fabricated Fe_2O_3NPs

3.3. Antileishmanial Potential

To evaluate the antileishmanial activity, the prepared NPs were tested at various concentrations over 72 h, and their effectiveness is shown in Figure 4. The quantity of promastigotes was determined in both NPs-amended and control groups at different time points: 24, 36, 48, and 72 h. The antileishmanial activity increased with higher concentrations of Fe_2O_3NPs. After 24 h of incubation, the antileishmanial effects were 20%, 32%, 35%, and 39% at 25, 50, 100, and 200 µg/mL, respectively. After 36 h, the Fe_2O_3NPs showed efficacy of 30%, 34%, 39%, and 50% at the same concentrations. After 48 h of incubation, the inhibition rates were 38% at 25 µg/mL, 52% at 50 µg/mL, 62% at 100 µg/mL, and 71% at 200 µg/mL. A slight reduction in the antileishmanial effect was observed thereafter, which may be attributed to the depletion of reactive oxygen species (ROS) produced by the Fe_2O_3NPs. The slight decline at later stages suggests that continuous ROS production is critical for sustaining the maximum anti-leishmanicidal activity, and depletion of ROS or aggregation of nanoparticles may reduce efficacy [58]. Similar findings have been reported for other metal oxide

JOURNAL FOR SOCIAL SCIENCE STUDIES
An International Peer-Reviewed Open Access Journal
ISSN (Online): 3006-2071 | ISSN (Print): 3006-2063
Volume 4 • Issue 4 • August 2026

nanoparticles, where oxidative stress and membrane damage were the primary modes of parasite inhibition [59]. Fe_2O_3NPs can generate reactive ions that form holes in the pathogen's cell wall, disrupt membrane structure, cause seepage of intracellular materials, and ultimately lead to pathogen destruction. The significant results of this study suggest that Fe_2O_3NPs could be a promising tool for treating leishmaniasis, which is consistent with previous research [60]. These observations highlight that *Moringa oleifera*-mediated Fe_2O_3NPs combine both the metallic core activity and the phytochemical contribution, making them superior candidates for leishmanicidal applications [61].

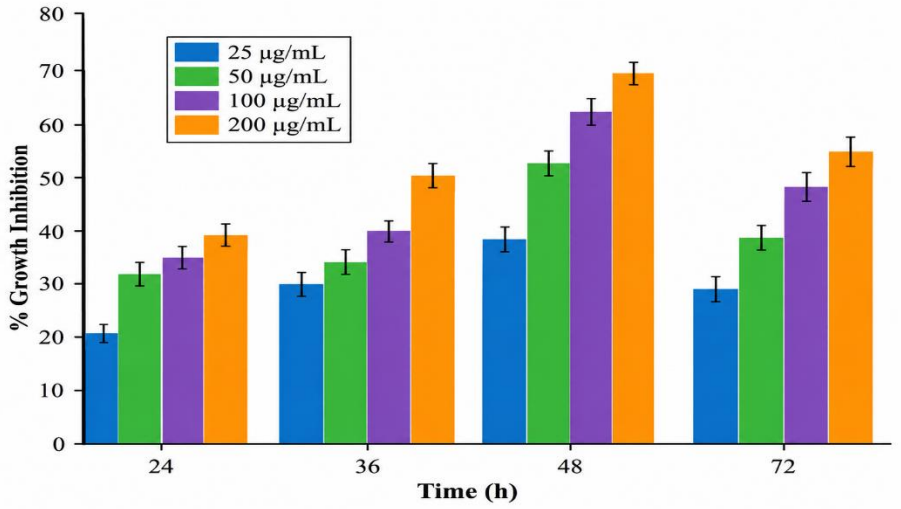

Figure 4. Antileishmanial activity of phyto-fabricated Fe_2O_3NPs at different concentrations.

3.4. Anti-Inflammatory potential

The synthesized Fe_2O_3NPs demonstrated effective anti-inflammatory properties (Figure 5). The Fe_2O_3NPs helped reduce inflammation at various concentrations. The highest anti-inflammatory effect was observed after 48 h of incubation, with inhibition rates of 55% at 25 µg/mL, 60% at 50 µg/mL, 63% at 100 µg/mL, 70% at 200 µg/mL, and 79% at 400 µg/mL. Further incubation beyond 48 h did not result in more than 79% inhibition. A comparative analysis showed that Fe_2O_3NPs were more effective as an anti-inflammatory agent at specific concentrations. These results are consistent with previous studies [62,63]. The anti-inflammatory response may be attributed to the ability of Fe_2O_3 NPs to inhibit protein denaturation and stabilize membrane proteins, which are key events in the inflammatory cascade [64]. Phytochemicals adsorbed on the surface of the nanoparticles could also synergize with iron oxide to enhance suppression of pro-inflammatory mediators [65]. Additionally, the dose-dependent activity suggests that higher concentrations of Fe_2O_3NPs provide stronger protection against protein denaturation and tissue damage. These findings support the potential of biosynthesized Fe_2O_3NPs as alternative therapeutic agents for managing inflammation-related disorders.

JOURNAL FOR SOCIAL SCIENCE STUDIES
An International Peer-Reviewed Open Access Journal

ISSN (Online): 3006-2071 | ISSN (Print): 3006-2063
Volume 4 • Issue 4 • August 2026

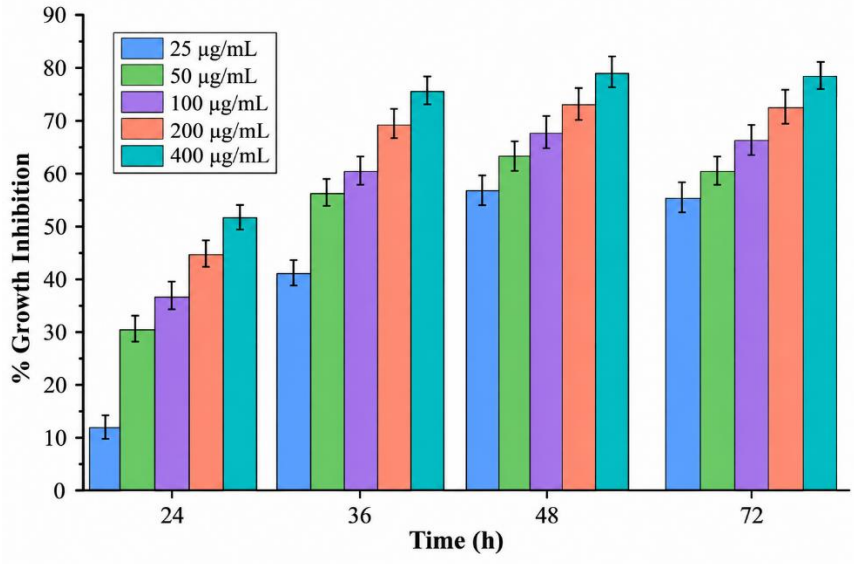

Figure 5. Anti-inflammatory activity of phyto-fabricated Fe_2O_3NPs at different concentrations.

3.5. Antioxidant activity

The antioxidant efficacy of Fe_2O_3NPs was evaluated at different concentrations (50–200 µg/mL). The antioxidant activities, including TAC, DPPH, and TRP, are shown in Figure 6. The highest TAC value, measured in terms of AA equivalents per mg, was 78.4% for Fe_2O_3NPs at 200 µg/mL, confirming their ability to scavenge reactive oxygen species (ROS). TRP was conducted to further investigate the existence of antioxidant species associated with Fe_2O_3NPs, focusing on reductones that play a crucial part in antioxidant potential [66]. The highest TRP value (75.2%) was observed at 200 µg/mL. Additionally, the DPPH radical scavenging capacity reached 64.6% for Fe_2O_3NPs at 200 µg/mL. These results are consistent with the aforementioned studies on phyto-fabricated Fe_2O_3NPs [67]. Moreover, the strong antioxidant activities of Fe_2O_3NPs highlight their potential as effective agents in combating oxidative stress-related diseases. These findings suggest that Fe_2O_3NPs could be valuable in various therapeutic and biomedical applications where antioxidant properties are essential. Similar antioxidant efficiencies have been reported for green-synthesized Fe_2O_3, which also displayed high DPPH scavenging and TAC values [68]. However, unlike our Fe_2O_3NPs, some of these nanoparticles exhibited comparatively lower TRP values, suggesting differences in the phytochemical capping agents from plant extracts [69].

JOURNAL FOR SOCIAL SCIENCE STUDIES
An International Peer-Reviewed Open Access Journal
ISSN (Online): 3006-2071 | ISSN (Print): 3006-2063
Volume 4 • Issue 4 • August 2026

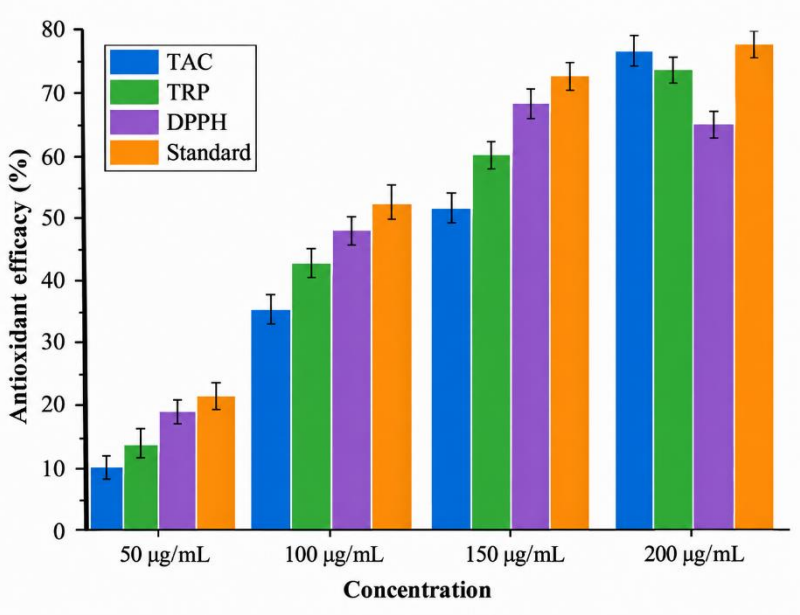

Figure 6. Antioxidant potential of phyto-fabricated Fe_2O_3NPs

3.6. Biocompatibility assay

The hemolytic test was designed to examine the toxicity of the Fe_2O_3NPs using RBCs. RBCs were mixed with Fe_2O_3NPs at concentrations ranging from 25 µg/mL to 200 µg/mL in a buffer solution prepared to simulate the extracellular environment. Ethical approval for the use of human blood samples was obtained from the institutional human ethics committee (Approval No.: 2024/R624); all procedures were conducted in accordance with relevant ethical guidelines. The assay is based on the principle that hemoglobin is released into the medium when RBCs lyse, which only occurs if the tested sample induces cell rupture. The consequences of the hemolytic assay are presented in Table 3. According to the American Society for Testing and Materials, materials with hemolysis greater than 2% are considered non-hemolytic, those with hemolysis between 2-5% are mildly hemolytic, and materials with hemolysis greater than 5% are classified as hemolytic [70]. The results indicate that the phyto-fabricated Fe_2O_3NPs displayed hemocompatibility, even at the highest dosage, with no significant hemolysis observed. The biocompatibility of these NPs is crucial for their potential biomedical applications. Consequently, our findings confirm the safety of the prepared NPs and support their use in therapeutic applications [71, 72]. Similar results were reported by Fouhma et al. (2019) [73], where green-synthesized Fe_2O_3NPs using *Helianthemum lippii* extract also showed excellent hemocompatibility with hemolysis below 2%. In contrast, iron oxide nanoparticles synthesized using *Cucurbita pepo* extract exhibited mild hemolytic activity above 100 µg/mL, differing from our findings [74]. These comparisons suggest that while biogenic Fe_2O_3NPs generally demonstrate blood compatibility, variations in plant phytochemicals can significantly influence hemolytic responses.

JOURNAL FOR SOCIAL SCIENCE STUDIES
An International Peer-Reviewed Open Access Journal

ISSN (Online): 3006-2071 | ISSN (Print): 3006-2063
Volume 4 • Issue 4 • August 2026

Table 3. % Hemolysis of plant-mediated Fe_2O_3NPs

S.NO	Concentration (µg/mL)	% Hemolysis
1	200	1.46±0.10
2	100	0.96±0.14
3	50	0.71±0.10
4	25	0.49±0.12

3.7. Protein Kinase (PK) Inhibition Assay

Protein kinase (PK) is essential in the development of anticancer therapies, as it phosphorylates serine-threonine and tyrosine residues that are involved in regulating multiple biological processes like cell growth, apoptosis, differentiation, and metabolism. Dysregulated phosphorylation can lead to genetic abnormalities, contributing to tumor formation. As a result, compounds capable of inhibiting PK are considered promising antitumor agents. In the present study, green-synthesized Fe_2O_3NPs were tested for their PK inhibition potential in the *Streptomyces 85E* strain, at a dosage rate ranging from 1.0 mg/mL to 16 mg/mL. Dose-dependent inhibition was observed with Fe_2O_3NPs treatments [74]. The largest zone of inhibition (ZOI) was recorded at 16 mg/mL, measuring 14.4 ± 1.22, while the smallest ZOI was 4.1 ± 1.0 at 1 mg/mL (Table 4). In Figure7, Series 1 represents the control group, while Series 2 shows the treatments at different concentrations. Additionally, prior studies on plant-based Fe_2O_3NPs have shown similar findings; for instance, Morgan et al. (2024) [75] reported comparable PK inhibition with metal oxide nanoparticles, while Abbasi et al. (2020) [76] observed variations using *Rhamnus triquetra* leaf extract-derived IONPs. These results highlight the potential of green-synthesized Fe_2O_3NPs as effective PK inhibitors, suggesting their role as promising candidates in cancer therapeutics. The observed dose-dependent activity further supports the relevance of Fe_2O_3NPs in modulating key enzymes involved in cancer progression.

Table 4. Protein Kinase Inhibition of phyto-fabricated Fe_2O_3NPs

Concentration (mg/mL)	Series 1 – Zone of Inhibition (mm)	Series 2 – Zone of Inhibition (mm)
1	4.0	5.7
2	6.7	7.7
4	8.7	8.7
8	11.7	12.1

JOURNAL FOR SOCIAL SCIENCE STUDIES
An International Peer-Reviewed Open Access Journal
ISSN (Online): 3006-2071 | ISSN (Print): 3006-2063
Volume 4 • Issue 4 • August 2026

Concentration (mg/mL)	Series 1 – Zone of Inhibition (mm)	Series 2 – Zone of Inhibition (mm)
16	14.3	14.8

3.8. Anti-diabetic Assay

Diabetes Mellitus (DM) is characterized by high glucose levels produced by inadequate production of insulin. Lowering postprandial hyperglycemia, which can be done through inhibiting AA and AG, which are vital glycan-hydrolyzing enzymes in the gastrointestinal tract, is one of the effective therapeutic approaches for DM [77]. In the current study, different doses of the prepared nanoparticles, ranging from 25 µg/mL to 400 µg/mL, were analyzed for AA and AG inhibition as depicted in Table 5. The highest inhibition was 55.23±0.35% calculated at 400 µg/mL for AA, whereas 56.59±1.34% for α-glucosidase, correspondingly. Our result confirms and supports the earlier described studies on Fe_2O_3NPs as AA and AG inhibitors. Such noteworthy anti-diabetic activity of Fe_2O_3NPs against diabetes enzymes may lead to new pharmacological strategies to cure DM [77]. Furthermore, the ability of Fe_2O_3NPs to regulate blood sugar levels by inhibiting these enzymes suggests their potential use as an adjunct therapy in diabetes management. The promising results from this study highlight the therapeutic potential of Fe_2O_3NPs in combating hyperglycemia and improving glucose control. Comparable antidiabetic potential has also been reported for *Moringa oleifera* extracts, including inhibition of α-amylase and α-glucosidase, supporting the relevance of *M. oleifera* phytochemicals to carbohydrate-metabolism assays [78]. In contrast, green-synthesized Fe_2O_3NPs using Cucurbita pepo extract exhibited lower inhibitory activity [74]. These variations suggest that differences in plant phytochemicals used for nanoparticle synthesis can significantly influence the antidiabetic efficacy of Fe_2O_3NPs.

Table 5. α-Glucosidase and α-amylase inhibition assay of phyto-fabricated Fe_2O_3NPs

Conc. µg/mL	α-amylase		α–glucosidase	
	Fe_2O_3NPs	Acarbose	Fe_2O_3NPs	Acarbose
400	55.23±0.35	83.30±1.33	56.59±1.34	83.45±1.83
200	38.12±0.52	73.60±1.62	40.26±0.29	64.50±1.76
100	28.51±0.38	54.53±1.18	26.59±0.35	59.31±1.22
50	19.14±0.36	35.47±0.84	18.44±0.23	35.34±1.34
25	15.15±0.25	35.38±0.77	13.43±0.34	29.42±0.68

3.9. Antimicrobial activity

3.9.1. In vitro antibacterial activity

In the current study, the efficiency of the prepared phyto-coated Fe_2O_3NPs was evaluated using *P. aeruginosa*, *S. aureus*, and *E. coli*. The overall

JOURNAL FOR SOCIAL SCIENCE STUDIES
An International Peer-Reviewed Open Access Journal
ISSN (Online): 3006-2071 | ISSN (Print): 3006-2063
Volume 4 • Issue 4 • August 2026

antibacterial efficiency of the Fe_2O_3NPs is summarized in Table 5. Each Fe_2O_3NPs dose (200, 100, 50 µg/mL) was applied to *P. aeruginosa*, *S. aureus*, and *E. coli*, and the ZOI was determined. The largest ZOI of 24.0 mm was observed at 200 µg/mL, followed by 19.0 mm at 100 µg/mL and 15.1 mm at 50 µg/mL for *E. coli* (Table 5). For *P. aeruginosa*, the highest ZOI was 22.0 mm at 200 µg/mL, followed by 17.0 mm at 100 µg/mL and 14.2 mm at 50 µg/mL. Against *S. aureus*, the ZOI was 21 mm at 200 µg/mL, 16 mm at 100 µg/mL, and 14 mm at 50 µg/mL (Table 6). In antibacterial trials, the bacterial membrane acts as the primary protective barrier against external agents.

Fe_2O_3 exhibits efficient antibacterial activity through multiple mechanisms. One of the prime mechanisms involves the reactive oxygen species (ROS) production, such as superoxide anions (O_2^-), hydroxyl radicals ($OH^·$), and hydrogen peroxide (H_2O_2) [79]. These ROS induce lipid peroxidation and oxidative stress, leading to DNA damage and protein denaturation. This leads to leakage of intracellular components and ultimately the death of the cell. Furthermore, the nanoscale size and high surface-to-volume ratio of Fe_2O_3 improve its ability to interact with bacterial cells, facilitating greater ion release, which can further interfere with essential cellular functions and enzyme activity [80]. The cell membrane is the first line of defense in an antibacterial trial, which protects the bacteria from foreign agents. Fe_2O_3 with a larger surface-to-volume ratio causes more production of more reactive ions. These reactive ions lead to DNA damage, protein lysis, enzyme breakdown, and finally cause bacterial death [77]. Loss of integrity of the cell membrane is considered the main reason for the bactericidal influence of Fe_2O_3 on *bacterial* cells [81, 82]. Our results are in good agreement with previous related studies of Jamzad *et al.* (2020) [83], who worked on the aqueous extract of *Laurus nobilis* L. leaves.

Table 6. Antibacterial activity of phyto-fabricated Fe_2O_3NPs (50 µg/mL, 100 µg/mL & 200 µg/mL

S. No.	Bacterial Species	Positive control (in mm) (CRO)	Negative control (DMSO)	Methanol Extract		
				Zone of Inhibition (mm)		
				50 µg/mL	100 µg/mL	200 µg/mL
1	***Escherichia coli***	30 ± 1.22**	0	15.1 ± 1.11*	19 ± 1.22*	24 ± 1.44*
2	***Pseudomonas aeruginosa***	31 ± 0.55	0	14.2 ± 0.77*	17 ± 0.56*	22 ± 1.45*
3	***Staphylococcus aureus***	35 ± 1.33*	0	14.0 ± 0.88*	16 ± 0.66*	21 ± 0.26*

3.9.2. Antifungal efficacy

The antifungal potential of the bioinspired Fe_2O_3NPs was evaluated via Petri plates containing PDA (Figure 7). The maximum inhibition (70 ± 2.1%) was examined at a concentration of 1 mg/mL, followed by 0.75 mg/mL (59 ± 1.4%), 0.50 mg/mL (51.33 ± 0.5%), and 0.25 mg/mL (38.11± 0.5%) Increasing the Fe_2O_3NPs concentration beyond these doses did not lead to additional inhibition, possibly due to nanoparticle aggregation at higher concentrations. With their smaller size and larger surface area, Fe_2O_3NPs are more reactive and stable [84, 85]. Physicochemical factors, including Brownian movement, size, and surface charge, can also induce particle aggregation. Over the last decade, mycologists have successfully applied Fe_2O_3NPs to inhibit various pathogens (fungi), including *Candida albicans*, *Fusarium graminearum*, and *Aspergillus niger* [86, 87, 88]. It has been proposed that the antifungal potential of phyto-fabricated Fe_2O_3NPs is associated with the generation of ROS. Additionally, nanomaterials have been shown to strongly intermingle with microbial cell

JOURNAL FOR SOCIAL SCIENCE STUDIES
An International Peer-Reviewed Open Access Journal
ISSN (Online): 3006-2071 | ISSN (Print): 3006-2063
Volume 4 • Issue 4 • August 2026

walls, demonstrating antimicrobial effects [89]. Fe_2O_3NPs form apertures in the cell wall, disrupting the plasma membrane's configuration and causing changes in depolarization, elasticity, fluidity, and absorbency. This allows the Fe_2O_3NPs to enter the cytoplasm, where they disrupt DNA, RNA, and proteins [90]. Consequently, the leakage of cellular machinery, including RNA, proteins, DNA, and enzymes, occurs, leading to cell death.

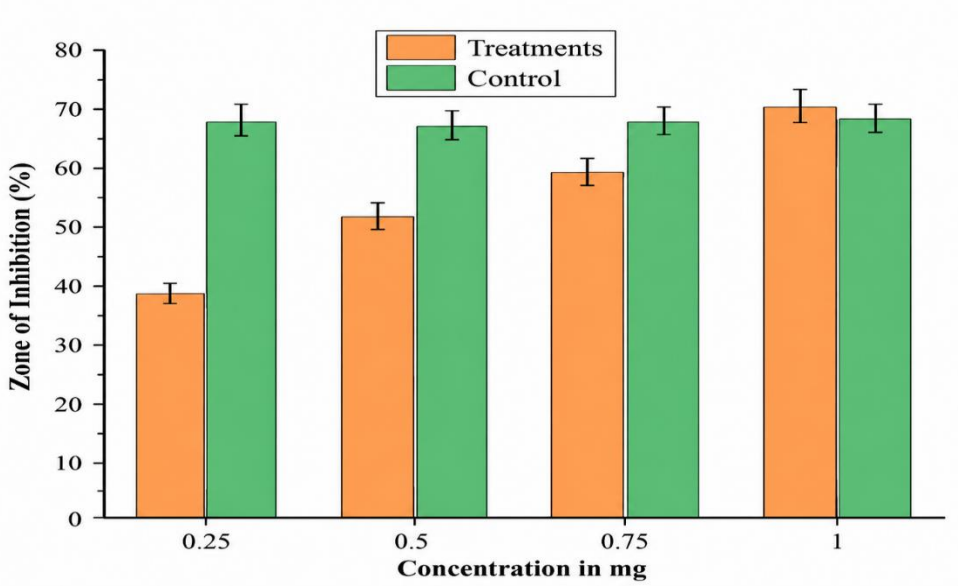

Figure 7. Antifungal potential control and treatment (0.25, 0.50, 0.75, and 1.0 mg/mL of phyto-fabricated Fe_2O_3NPs)

5. Conclusion

This study demonstrated the successful green synthesis of Fe_2O_3NPs using *Moringa oleifera*, confirming their structural integrity and multifunctional biological activities, including antimicrobial, antioxidant, anti-inflammatory, antidiabetic, and biocompatible properties. The integration of phytochemicals from *M. oleifera* not only acted as reducing and stabilizing agents but also contributed synergistically to the observed therapeutic potential of the nanoparticles. These findings emphasize the value of plant-mediated synthesis as a sustainable approach to produce bioactive nanomaterials with broad-spectrum applications. While these results highlight their promise for biomedical use, the current work is limited to in vitro evaluations. Future research should focus on optimizing synthesis for stability, scale-up production, and targeted delivery, alongside in vivo studies to assess pharmacokinetics, toxicity, and therapeutic efficacy. Such efforts are essential to translate these nanoparticles from laboratory findings to clinical and biomedical applications.

Abbreviations: Fe_2O_3NPs, DNA, RNA, ROS, ZOI, mm, µg/mL, RBCs, DPPH, EDX, SEM, FTIR, TRP, FRSA.

Declarations

Ethical Approval

The collection of plant material must comply with relevant institutional, national, and international guidelines and legislation. Our study complies with relevant institutional, national, and international guidelines and legislation.

Consent to Participate

Not applicable.

ISSN (Online): 3006-2071 | ISSN (Print): 3006-2063
Volume 4 • Issue 4 • August 2026

Consent to Publish
Not applicable.

Author declaration
All authors agree to publish the work in its current form.

Clinical Trial Number
Not applicable

Author Contributions
Khitab Ur Rahman: Conceptualization, methodology, investigation, data curation, formal analysis, and writing—original draft. Saqiba Riaz: Conceptualization, supervision, project administration, methodology, validation, and writing—review and editing. Muhammad Mohsin: Investigation, data collection, formal analysis, and writing—original draft. Mohammad Munir Akbar: Methodology, investigation, data curation, and formal analysis. Hazrat Bilal: Investigation, visualization, data analysis, and writing—review and editing. Rabail Urooj: Validation, visualization, literature review, and writing—review and editing. All authors read and approved the final version of the manuscript.

Funding: Not applicable

Competing Interest
The authors declare that they have no competing interests.

Availability of Data and Materials
All relevant data generated or analyzed during this study are included in this manuscript. Additional data may be made available upon reasonable request from the corresponding authors.

Acknowledgments
We are thankful to all the authors who participated in this research work.

REFERENCES

Sishu, N. K., Karunakaran, M. K. R., Hadkar, V. M., Mohanty, C., Sharmila, A., Selvaraj, C. I., & Babu, N. G. (2025). Phyto-mediated synthesis of SnO 2 nanoparticles using Croton malabaricus Bedd. for its antioxidant, antibacterial, hemocompatibility properties and photocatalytic activity. *New Journal of Chemistry*, *49*(2), 536-552.

Khatami, M.; Varma, R. S.; Zafarnia, N.; Yaghoobi, H.; Sarani, M.; Kumar, V. G. Applications Of green synthesized Ag, ZnO and Ag/ZnO nanoparticles for making clinical antimicrobial Wound healing bandages. *Sustain. Chem. and Pharm.* 2018, 10, 9-15.

Hachem, K., Ansari, M. J., Saleh, R. O., Kzar, H. H., Al-Gazally, M. E., Altimari, U. S., ... & Kianfar, E. (2022). Methods of chemical synthesis in the synthesis of nanomaterial and nanoparticles by the chemical deposition method: a review. *BioNanoScience*, *12*(3), 1032-1057.

Alavi, M., & Nokhodchi, A. (2021). Synthesis and modification of bio-derived antibacterial Ag and ZnO nanoparticles by plants, fungi, and bacteria. *Drug Discovery Today*, *26*(8), 1953-1962.

Kirubakaran, D. (2025). Review on Emerging Frontiers in Medical Sensing: Innovations Shaping the Future of Healthcare. *Biomedical Materials & Devices*, 1-21.

Gunalan, S., Sivaraj, R., & Rajendran, V. (2012). Green synthesized ZnO nanoparticles against bacterial and fungal pathogens. *Progress in Natural Science: Materials International*, *22*(6), 693-700.

ISSN (Online): 3006-2071 | ISSN (Print): 3006-2063
Volume 4 • Issue 4 • August 2026

Sabouri, Z., Sabouri, S., Moghaddas, S. S. T. H., Mostafapour, A., Gheibihayat, S. M., & Darroudi, M. (2022). Plant-based synthesis of Ag-doped ZnO/MgO nanocomposites using Caccinia macranthera extract and evaluation of their photocatalytic activity, cytotoxicity, and potential application as a novel sensor for detection of Pb2+ ions. *Biomass Conversion and Biorefinery*, 1-13.

Tariq, M., Mohammad, K. N., Ahmed, B., Siddiqui, M. A., & Lee, J. (2022). Biological synthesis of silver nanoparticles and prospects in plant disease management. *Molecules*, *27*(15), 4754.

Hadkar, V. M., Sishu, N. K., Jayabharathi, S. P., Sharmila, A., & Selvaraj, C. I. (2025). Biogenic synthesis of Albizia lucidior mediated magnetite nanoparticles (Fe3O4 NPs): Therapeutic applications and photocatalytic activity. *Biocatalysis and Agricultural Biotechnology*, 103676.

Guerrini, L., Alvarez-Puebla, R. A., & Pazos-Perez, N. (2018). Surface modifications of nanoparticles for stability in biological fluids. *Materials*, *11*(7), 1154.

Ali, A., Phull, A. R., & Zia, M. (2018). Elemental zinc to zinc nanoparticles: Is ZnO NPs crucial for life? Synthesis, toxicological, and environmental concerns. *Nanotechnology Reviews*, *7*(5), 413-441.

Papitha, R., Hadkar, V., Sishu, N. K., Arunagiri, S., Roopan, S. M., & Selvaraj, C. I. (2024). Green synthesis of CuO/TiO2 and ZnO/TiO2 nanocomposites using Parkia timoriana bark extract: Enhanced antioxidant and antidiabetic activities for biomedical applications. *Ceramics International*, *50*(20), 39109-39121.

Noqta, O. A., Aziz, A. A., Usman, I. A., & Bououdina, M. (2019). Recent advances in iron oxide nanoparticles (IONPs): synthesis and surface modification for biomedical applications. *Journal of Superconductivity and Novel Magnetism*, *32*, 779-795.

Baabu, P. R. S., Kumar, H. K., Gumpu, M. B., Babu K, J., Kulandaisamy, A. J., & Rayappan, J. B. B. (2022). Iron Oxide Nanoparticles: A Review on the Province of Its Compounds, Properties and Biological Applications. *Materials*, *16*(1), 59.

Ansari, K., Ahmad, R., Tanweer, M. S., & Azam, I. (2024). Magnetic iron oxide nanoparticles as a tool for the advancement of biomedical and environmental application: a review. *Biomedical Materials & Devices*, *2*(1), 139-157.

Priya, Naveen, Kaur, K., & Sidhu, A. K. (2021). Green synthesis: An eco-friendly route for the synthesis of iron oxide nanoparticles. *Frontiers in Nanotechnology*, *3*, 655062.

Kirubakaran, D. (2025). Herbal remedies for Alzheimer's disease: Neuroprotective mechanisms and cognitive enhancement potential. *Digital Chinese Medicine*, *8*(2), 183-195.

Saini, R. K., Sivanesan, I., & Keum, Y.-S. (2016). Phytochemicals of Moringa oleifera: a review of their nutritional, therapeutic and industrial significance. 3 Biotech, 6, 203. https://doi.org/10.1007/s13205-016-0526-3.

Abd Rani, N. Z., Husain, K., & Kumolosasi, E. (2018). Moringa Genus: A Review of Phytochemistry and Pharmacology. Frontiers in Pharmacology, 9, 108. https://doi.org/10.3389/fphar.2018.00108.

ISSN (Online): 3006-2071 | ISSN (Print): 3006-2063
Volume 4 • Issue 4 • August 2026

Anwar, T., Qureshi, H., Sarwar, G., Siddiqi, E. H., Shakir, N., Almoallim, H. S., & Ansari, M. J. (2024). Ethnobotanical evaluation and Traditional uses of medicinal flora used to treat various ailments by local inhabitants. *Advances in Integrative Medicine*, *11*(2), 93-106.

Stohs, S. J., & Hartman, M. J. (2015). Review of the Safety and Efficacy of Moringa oleifera. Phytotherapy Research, 29(6), 796–804. https://doi.org/10.1002/ptr.5325.

Blundell, R., et al. (2024). A comprehensive review of the phytochemicals, health benefits, pharmacological safety and medicinal prospects of Moringa oleifera. Heliyon, 10, e27807. https://doi.org/10.1016/j.heliyon.2024.e27807.

Kayani, S., Ahmad, M., Zafar, M., Sultana, S., Khan, M. P. Z., Ashraf, M. A., ... & Yaseen, G. (2014). Ethnobotanical uses of medicinal plants for respiratory disorders among the inhabitants of Gallies–Abbottabad, Northern Pakistan. *Journal of ethnopharmacology*, *156*, 47-60.

Gupta, P. C., Sharma, N., & Rao, C. V. (2012). A review on ethnobotany, phytochemistry and pharmacology of Fumaria indica (Fumitory). *Asian Pacific Journal of Tropical Biomedicine*, *2*(8), 665-669.

de Moura Barbosa, H., Amaral, D., do Nascimento, J. N., Machado, D. C., de Sousa Araújo, T. A., de Albuquerque, U. P., ... & Lira, E. C. (2018). Spondias tuberosa inner bark extract exert antidiabetic effects in streptozotocin-induced diabetic rats. *Journal of ethnopharmacology*, *227*, 248-257.

Shaikh, J. R., & Patil, M. (2020). Qualitative tests for preliminary phytochemical screening: An overview. *International journal of chemical studies*, *8*(2), 603-608.

Bukhari, I. A., Khan, R. A., Gilani, A. H., Ahmed, S., & Saeed, S. A. (2010). Analgesic, anti-inflammatory and anti-platelet activities of the methanolic extract of Acacia modesta leaves. *Inflammopharmacology*, *18*, 187-196.

Abdullah, J. A. A., Eddine, L. S., Abderrhmane, B., Alonso-González, M., Guerrero, A., & Romero, A. (2020). Green synthesis and characterization of iron oxide nanoparticles by pheonix dactylifera leaf extract and evaluation of their antioxidant activity. *Sustainable Chemistry and Pharmacy*, *17*, 100280.

Alexeree, S. M., Abou-Seri, H. M., El-Din, H. E. S., Youssef, D., & Ramadan, M. A. (2024). Green synthesis of silver and iron oxide nanoparticles mediated photothermal effects on Blastocystis hominis. *Lasers in Medical Science*, *39*(1), 43.

Shah, A., Sun, H., Qiao, Z., Khan, M. U., Ali, N., Gao, C., ... & Kashif, M. (2024). Synthesis of Iron Oxide Nanoparticles and its Antimicrobial, Anticancer, Anti-inflammatory, Wound Healing, and Immunomodulatory Activities-A Review. *Phytopharmacology Research Journal*, *3*(3), 1-28.

Mthana, M. S., Mthiyane, D. M., Onwudiwe, D. C., & Singh, M. (2022). Biosynthesis of ZnO nanoparticles using capsicum Chinense fruit extract and their in vitro cytotoxicity and antioxidant assay. *Applied Sciences*, *12*(9), 4451.

Nayak, D., Mishra, A. K., Malla, S., Swain, U., Panigrahi, K., Panda, J., ... & Mohanta, Y. K. (2024). Eco-friendly mycogenic synthesis of iron oxide nanoparticles using Volvariella volvacea and unveiling its potential as antibiofilm and anticancer agents. *ECS Journal of Solid State Science and Technology*, *13*(8), 087003.

ISSN (Online): 3006-2071 | ISSN (Print): 3006-2063
Volume 4 • Issue 4 • August 2026

Srikar, S. K., Giri, D. D., Pal, D. B., Mishra, P. K., & Upadhyay, S. N. (2016). Green synthesis of silver nanoparticles: a review. *Green and Sustainable Chemistry*, *6*(1), 34-56.

Ibrahim, M. M., Zaki, E. R., & Rady, M. R. (2024). Alpha-amylase inhibitory activity and in silico studies of in vitro sweet basil plantlets treated with chitosan and ZnO NPs. *In Vitro Cellular & Developmental Biology-Plant*, 1-14.

Das, S. K., Behera, S., Patra, J. K., & Thatoi, H. (2019). Green synthesis of sliver nanoparticles using Avicennia officinalis and Xylocarpus granatum extracts and in vitro evaluation of antioxidant, antidiabetic and anti-inflammatory activities. *Journal of Cluster Science*, *30*, 1103-1113.

Rafique, M., Sadaf, I., Rafique, M. S., & Tahir, M. B. (2017). A review on green synthesis of silver nanoparticles and their applications. *Artificial cells, nanomedicine, and biotechnology*, *45*(7), 1272-1291.

Buarki, F., AbuHassan, H., Al Hannan, F., & Henari, F. Z. (2022). Green synthesis of iron oxide nanoparticles using Hibiscus rosa sinensis flowers and their antibacterial activity. *Journal of Nanotechnology*, *2022*(1), 5474645.

Malik, A., et al. (2021). Anticancer activities of phenolic compounds from Moringa oleifera leaves: in vitro and in silico mechanistic study. Beni-Suef University Journal of Basic and Applied Sciences. https://doi.org/10.1186/s43088-021-00101-2.

Kirubakaran, D. (2025). Herbal remedies for Alzheimer's disease: neuroprotective mechanisms and cognitive enhancement potential. *Digital Chinese Medicine*, *8*(2), 183-195.

Kirubakaran, D., & Krishnan, V. (2025). Toxicological profile and therapeutic potentials of Impatiens chinensis leaf extract: Exploring antibacterial, antioxidant, antidiabetic and insecticidal properties. *Pharmacological Research-Natural Products*, *7*, 100238.

Goudjil, M. B., Dali, H., Zighmi, S., Hamada, D., Mahcene, Z., & Bencheikh, S. E. (2025). Successive photocatalytic degradation of methylene blue by CuO, Fe2O3, and novel nanocomposite CuO/Fe2O3 synthesized from Mentha pulegium plant extract via biosynthesis technique. *Biomass Conversion and Biorefinery*, *15*(2), 2557-2569.

Al-Karagoly, H., Rhyaf, A., Naji, H., Albukhaty, S., AlMalki, F. A., Alyamani, A. A., ... & Aloufi, S. (2022). Green synthesis, characterization, cytotoxicity, and antimicrobial activity of iron oxide nanoparticles using Nigella sativa seed extract. *Green Processing and Synthesis*, *11*(1), 254-265.

Chakraborty, A. R., Toma, F. T. Z., Alam, K., Yousuf, S. B., & Hossain, K. S. (2024). Influence of annealing temperature on Fe_2O_3 nanoparticles: Synthesis optimization and structural, optical, morphological, and magnetic properties characterization for advanced technological applications. *Heliyon*, *10*(21).

Ioncica, M. C., Bandyopadhyay, S., Bali, N., Socoliuc, V., & Bernad, S. I. (2023). Investigation of cubic and spherical IONPs' rheological characteristics and aggregation patterns from the perspective of magnetic targeting. *Magnetochemistry*, *9*(4), 99.

ISSN (Online): 3006-2071 | ISSN (Print): 3006-2063
Volume 4 • Issue 4 • August 2026

Shanmugarathinam, A., Elamaran, N., Kirubakaran, D., Irulappan, G. B., Baig, A. A., & Vasantharaj, K. (2025). Sustainable synthesis of zinc oxide nanoparticles from Vicoa indica leaf extract: Characterization and evaluation of antibacterial, antioxidant, and anticancer properties. *Biomedical Materials & Devices*, 1-16.

Hadkar, V. M., & Selvaraj, C. I. (2025). Characterization and investigating the potential therapeutic effects of phyto-assisted CuO and Zn-doped CuO nanoparticles from Calophyllum apetalum (Willd.) leaf extract. *Journal of Drug Delivery Science and Technology*, *104*, 106530.

Thakur, V., Narula, D., Sharma, A., Kaur, M., & Sharma, P. (2023). Investigation on green synthesized nanocomposites of magnetite using Salvia hispanica for antibacterial activity. *Materials Today: Proceedings*.

Jothibas, M., Paulson, E., Srinivasan, S., & Kumar, B. A. (2022). The impacts of interfacing phytochemicals on the structural, optical and morphology of hematite nanoparticles. *Surfaces and Interfaces*, *29*, 101734.

Javed, R., Zia, M., Naz, S., Aisida, S. O., Ain, N. U., & Ao, Q. (2020). Role of capping agents in the application of nanoparticles in biomedicine and environmental remediation: recent trends and future prospects. *Journal of Nanobiotechnology*, *18*(1), 172.

Singh, H., Desimone, M. F., Pandya, S., Jasani, S., George, N., Adnan, M., ... & Alderhami, S. A. (2023). Revisiting the green synthesis of nanoparticles: uncovering influences of plant extracts as reducing agents for enhanced synthesis efficiency and its biomedical applications. *International journal of nanomedicine*, 4727-4750.

Ansari, M. A., & Asiri, S. M. M. (2021). Green synthesis, antimicrobial, antibiofilm and antitumor activities of superparamagnetic γ-Fe2O3 NPs and their molecular docking study with cell wall mannoproteins and peptidoglycan. *International Journal of Biological Macromolecules*, *171*, 44-58.

Sharma, R., Garg, R., Bali, M., & Eddy, N. O. (2023). Potential applications of green-synthesized iron oxide NPs for environmental remediation. *Environmental Monitoring and Assessment*, *195*(11), 1397.

Talbot, D., Queiros Campos, J., Checa-Fernandez, B. L., Marins, J. A., Lomenech, C., Hurel, C., ... & Bee, A. (2021). Adsorption of organic dyes on magnetic iron oxide nanoparticles. Part I: Mechanisms and adsorption-induced nanoparticle agglomeration. *ACS omega*, *6*(29), 19086-19098.

Fahmy, H. M., Aly, E. M., Mohamed, F. F., Noor, N. A., & Elsayed, A. A. (2020). Neurotoxicity of green-synthesized magnetic iron oxide nanoparticles in different brain areas of wistar rats. *Neurotoxicology*, *77*, 80-93.

Borowska, M., & Jankowski, K. (2023). Basic and advanced spectrometric methods for complete nanoparticles characterization in bio/eco systems: current status and future prospects. *Analytical and Bioanalytical Chemistry*, *415*(18), 4023-4038.

Dubey, S.P.; Dwivedi, A.D.; Lahtinen, M.; Lee, C.; Kwon, Y.N.; Sillanpaa, M. Protocol for development of various plants leaves extract in single-pot synthesis of metal nanoparticles. Spectrochim. Acta Part A Mol. Biomol. Spectrosc. 2013, 103, 134–142.

ISSN (Online): 3006-2071 | ISSN (Print): 3006-2063
Volume 4 • Issue 4 • August 2026

Singh, K.; Chopra, D.S.; Singh, D.; Singh, N. Optimization and ecofriendly synthesis of iron oxide nanoparticles as potential antioxidant. Arab. J. Chem. 2020, 13, 9034–9046.

Gomathi, M., Kirubakaran, D., & Malarkodi, R. (2025). Synthesis, Characterization and Biomedical Environmental Applications of Magnesium-Doped Zinc Oxide Nanoparticles Using Laggera alata Extract. *Biomedical Materials & Devices*, 1-19.

Yousaf, R., Khan, M. A., Raza, A., Ambreen, Ali, H., Darwish, H., ... & Noureldeen, A. (2025). Iron oxide nanoparticles and light intensity modulate biomass, antioxidant capacity and anti-leishmanial activity in callus cultures of Artemisia scoparia. *Plant Cell, Tissue and Organ Culture (PCTOC)*, *160*(2), 27.

Sumaira, Siddique Afridi, M., Salman Hashmi, S., Ali, G. S., Zia, M., & Haider Abbasi, B. (2018). Comparative antileishmanial efficacy of the biosynthesised ZnO NPs from genus Verbena. *IET nanobiotechnology*, *12*(8), 1067-1073.

Abbasi, B. A., Iqbal, J., Mahmood, T., Qyyum, A., & Kanwal, S. (2019). Biofabrication of iron oxide nanoparticles by leaf extract of Rhamnus virgata: Characterization and evaluation of cytotoxic, antimicrobial and antioxidant potentials. *Applied Organometallic Chemistry*, *33*(7), e4947.

Grosse, S., Stenvik, J., & Nilsen, A. M. (2016). Iron oxide nanoparticles modulate lipopolysaccharide-induced inflammatory responses in primary human monocytes. *International journal of nanomedicine*, 4625-4642.

Khoobi, A., Soltani, N., & Aghaei, M. (2020). Computational design and multivariate statistical analysis for electrochemical sensing platform of iron oxide nanoparticles in sensitive detection of anti-inflammatory drug diclofenac in biological fluids. *Journal of Alloys and Compounds*, *831*, 154715.

Shah, A., Sun, H., Qiao, Z., Khan, M. U., Ali, N., Gao, C., ... & Kashif, M. (2024). Synthesis of Iron Oxide Nanoparticles and its Antimicrobial, Anticancer, Anti-inflammatory, Wound Healing, and Immunomodulatory Activities-A Review. *Phytopharmacology Research Journal*, *3*(3), 1-28.

Gomathi, M., Kirubakaran, D., & Malarkodi, R. (2025). Synthesis, Characterization and Biomedical Environmental Applications of Magnesium-Doped Zinc Oxide Nanoparticles Using Laggera alata Extract. *Biomedical Materials & Devices*, 1-19.

Alqarni, Z. (2024). Enhanced Antibiotic Degradation and Antioxidant Activity Using a Novel Biosynthesized PVP-Modified Fe2O3/Fe3O4 Nanocomposite: A Dual Approach to Environmental and Human Health. *Journal of Cluster Science*, *35*(6), 1845-1860.

Kirubakaran, D., & Krishnan, V. (2025). Toxicological profile and therapeutic potentials of Impatiens chinensis leaf extract: Exploring antibacterial, antioxidant, antidiabetic and insecticidal properties. *Pharmacological Research-Natural Products*, *7*, 100238.

Ashrafi-Saiedlou, S., Rasouli-Sadaghiani, M., & Fattahi, M. (2025). Green synthesis of iron oxide nanoparticles using Thymus migricus for multifunctional applications in antioxidant, antimicrobial, photocatalytic, and seed priming processes. *Heliyon*, *11*(5).

ISSN (Online): 3006-2071 | ISSN (Print): 3006-2063
Volume 4 • Issue 4 • August 2026

Hilo, D. H., Ismail, A. H., & Al-Garawi, Z. S. (2022). Green synthesis of A-Fe2O3 from ginger extract enhanced the potential antioxidant activity against DPPH. *Al-Mustansiriyah Journal of Science*, *33*(4), 64-71.

Anamaghi, P. N., & Kouchakzadeh, H. (2019). BSA nanoparticles loaded with IONPs for biomedical applications: fabrication optimization, physicochemical characterization and biocompatibility evaluation. *Nanomedicine Journal*, *6*(1).

Kirubakaran, D., Wahid, J. B. A., Karmegam, N., Jeevika, R., Sellapillai, L., Rajkumar, M., & SenthilKumar, K. J. (2025). A comprehensive review on the green synthesis of nanoparticles: advancements in biomedical and environmental applications. *Biomedical Materials & Devices*, 1-26.

Kirubakaran, D. (2025). Review on Emerging Frontiers in Medical Sensing: Innovations Shaping the Future of Healthcare. *Biomedical Materials & Devices*, 1-21.

Fouhma, A., Tamma, N., Rebiai, A., & Bouafia, A. (2024). Comprehensive study on antibacterial, antioxidant, and photocatalytic activity of iron oxide nanoparticles synthesized using Helianthemum lippii (L.) pers. *Journal of Sol-Gel Science and Technology*, 1-21.

Gula, H., Khan, H. A., Nasreen, Z., Assad, N., Turab, S. A., & Hanif, M. (2025). Exploring the Antibacterial, Anticoagulant, and Hemolytic Potential of Green-Synthesized Fe 2 O 3 Nanoparticles by Cucurbita pepo pulp. *IEEE Transactions on NanoBioscience*.

Morgan, R. N., & Aboshanab, K. M. (2024). Green biologically synthesized metal nanoparticles: biological applications, optimizations and future prospects. *Future Science OA*, *10*(1), FSO935.

Abbasi, B. A., Iqbal, J., Zahra, S. A., Shahbaz, A., Kanwal, S., Rabbani, A., & Mahmood, T. (2020). Bioinspired synthesis and activity characterization of iron oxide nanoparticles made using Rhamnus Triquetra leaf extract. *Materials Research Express*, *6*(12), 1250e7.

Hola, K., Markova, Z., Zoppellaro, G., Tucek, J., & Zboril, R. (2015). Tailored functionalization of iron oxide nanoparticles for MRI, drug delivery, magnetic separation and immobilization of biosubstances. *Biotechnology advances*, *33*(6), 1162-1176.

Magaji, U. F., Sacan, O., & Yanardag, R. (2020). Alpha amylase, alpha glucosidase and glycation inhibitory activity of Moringa oleifera extracts. South African Journal of Botany, 128, 225–230. https://doi.org/10.1016/j.sajb.2019.11.024.

Xu, Y., Xiao, L., Chen, J., Wu, Q., Yu, W., Zeng, W., ... & Liu, Y. (2022). α-Fe2O3 based nanotherapeutics for near-infrared/dihydroartemisinin dual-augmented chemodynamic antibacterial therapy. Acta Biomaterialia, 150, 367-379.

Pourmadadi, M., Rahmani, E., Shamsabadipour, A., Mahtabian, S., Ahmadi, M., Rahdar, A., & Díez-Pascual, A. M. (2022). Role of iron oxide (Fe2O3) nanocomposites in advanced biomedical applications: a state-of-the-art review. *Nanomaterials*, *12*(21), 3873.

Das, S., Diyali, S., Vinothini, G., Perumalsamy, B., Balakrishnan, G., Ramasamy, T., ... & Biswas, B. (2020). Synthesis, morphological analysis, antibacterial activity of iron oxide nanoparticles and the cytotoxic effect on lung cancer cell line. *Heliyon*, *6*(9).

ISSN (Online): 3006-2071 | ISSN (Print): 3006-2063
Volume 4 • Issue 4 • August 2026

Fatih, H. J., Ashengroph, M., Sharifi, A., & Zorab, M. M. (2024). Green-synthesized α-Fe2O3-nanoparticles as potent antibacterial, anti-biofilm and anti-virulence agent against pathogenic bacteria. *BMC microbiology*, *24*(1), 535.

Jamzad, M., & Kamari Bidkorpeh, M. (2020). Green synthesis of iron oxide nanoparticles by the aqueous extract of Laurus nobilis L. leaves and evaluation of the antimicrobial activity. *Journal of nanostructure in Chemistry*, *10*(3), 193-201.

Nosrati, H., Salehiabar, M., Fridoni, M., Abdollahifar, M. A., Kheiri Manjili, H., Davaran, S., & Danafar, H. (2019). New insight about biocompatibility and biodegradability of iron oxide magnetic nanoparticles: stereological and in vivo MRI monitor. *Scientific reports*, *9*(1), 7173.

Yang, Bujun, M. Zang, M Wu, H. Zang, 2019. Synthesis of biochar-based Cu2O nanoparticles and their antibacterial activity against Escherichia coli. Inorg. Nano-Met. Chem. 49(1):12-16.

Hoseinzadeh, Abolghasem, Aziz Habibi-Yangjeh, and Mahdi Davari 2016. Antifungal activity of magnetically separable Fe3O4/ZnO/AgBr nanocomposites prepared by a facile microwave-assisted method. Prog. Nat. Sci. Mater. Int. 26(4):334-340.

Nguyen, Van Thang, et al. 2019. Antibacterial activity of TiO2-and ZnO-decorated with silver nanoparticles. J. Compos. Sci. 3(2):61.

Al-Karagoly, H., Rhyaf, A., Naji, H., Albukhaty, S., AlMalki, F. A., Alyamani, A. A., ... & Aloufi, S. (2022). Green synthesis, characterization, cytotoxicity, and antimicrobial activity of iron oxide nanoparticles using Nigella sativa seed extract. *Green Processing and Synthesis*, *11*(1), 254-265.

Ye, Y., He, J., Wang, H., Li, W., Wang, Q., Luo, C., ... & Zhou, M. (2022). Cell wall destruction and internal cascade synergistic antifungal strategy for fungal keratitis. *ACS nano*, *16*(11), 18729-18745.

Kamal, Asif, Urooj Haroon, Hakim Manghwar, Khalid H. Almer, Ibtisam M. Alsudas, Ashwaq T. Althobaiti, Anila Iqbal, Mahnoor Akbar, Farhana, Maryam Anar, Moona Nazish, Hassan Javed Chaudhary, Muhammad Farooq Hussain Munis, 2022. Biological Applications of Ball-Milled Synthesized Biochar-Zinc Oxide Nanocomposite Using Zea mays L. Molecules 27(16):5333.